A Numerical Experiment on a Disturbance in the Tropical Easterlies*

By J. Shukla

Institute of Tropical Meteorology, Poona

(*Manuscript received 9 October 1968, in revised form 14 January 1969*)

Abstract

A numerical experiment has been performed on a tropical disturbance embedded in easterlies to test the dependency of the vertical coupling on the value of Richardson number in tropics. By a 2-layer primitive equation model in sigma system of coordinates integrations have been performed for a period of 24 hours with two different sets of initial conditions in which the three dimensional structure of the initial easterly pattern is specified through pre-specified wind shear and different values of the Richardson number. The order of magnitude of vertical velocities, the time rate of change of kinetic energy and the phase speed of the disturbances is discussed for both the cases.

The preliminary results indicate that, even the tropical motions have appreciable degree of vertical coupling and baroclinic nature in the cases of low Richardson number. The results seem to be of special interest in context of the fact that even the mean monthly values of static stability during summer are found to be very small and even negative in the middle and lower troposphere in the tropics.

1. Introduction

A few years ago, Charney (1963) pointed out that for the same length, velocity and stability scales vertical velocity is much smaller at low latitudes than at high latitudes because in tropics the Rossby number is not small.

The expression for estimating the order of magnitude of vertical velocity W when $R_0 \ll 1$ is given as (Charney, 1963).

$$\frac{W}{D} \sim \frac{U}{L} \cdot \frac{1}{R_i} \cdot \frac{1}{R_0} \tag{1}$$

where L, D and U are respectively the characteristic parameters for horizontal scale, vertical scale and horizontal velocity. R_0 is Rossby number, R_i is Richardson number. However, for $R_0 \geq 1$

$$\frac{W}{D} \sim \frac{U}{L} \cdot \frac{1}{R_i} \tag{2}$$

Charney further concluded that the governing equation for tropics is the barotropic vorticity equation. However, the conclusion regarding barotropic nature of the tropical atmosphere may not be quite valid in the tropics in view of the fact that the Richardson number which depends inter alia on the static stability can be quite small, or even negative during certain periods when the equivalent potential temperature decreases with height (Yanai 1961, 1964: Rao 1958). On account of the abundance of moisture in the tropics especially in oceanic regions where tropical disturbances form, it appears more appropriate to use the equivalent potential temperature in determining static stability than the potential temperature. Here, the effect of the smallness of the value of the coriolis parameter may be outweighed by that of the smallness of the values of the Richardson number and, therefore, the vertical velocity in the tropics may be comparable or even more than that of the middle latitudes.

The existence of large scale vertical velocities in the tropical atmosphere is also evidenced by large amounts of rainfall which are observed over extensive areas in many parts of the tropical belt.

The aim of the present study is to examine the nature of the model disturbances, characterized by high and low values of Richardson number in the model tropical atmosphere. In specifying the different values of the Richardson number, the vertical wind shear has been kept constant and the static stability only has been varied. With this simplification, high and low values of Richardson number mean high and low values of static stability i.e. ($R_i \approx S$).

This investigation has been carried out with a

2-level primitive equation model in σ system of coordinates (Fig. 1).

$$\sigma = \frac{P - P_T}{P_S - P_T} \quad ; \quad P_T = 200 mb$$

p = 200mb ——————————————— $\sigma = 0.0$

U, V, T, ϕ $\sigma = 0.25$

$\dot{\sigma}, (\omega), \phi$ $\sigma = 0.5$

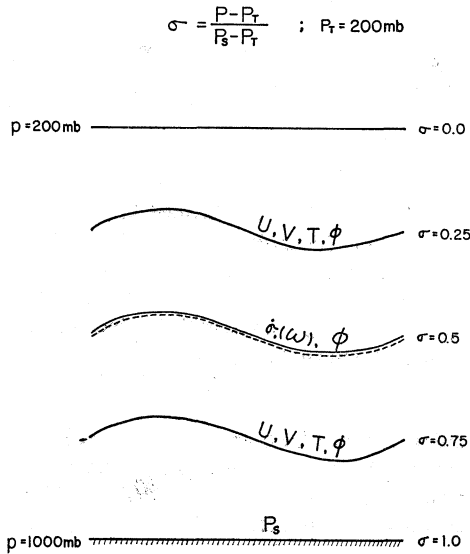U, V, T, ϕ $\sigma = 0.75$

p = 1000mb P_s $\sigma = 1.0$

Fig. 1. Schematic representation of vertical structure of the 2-level primitive equation model.

2. Initialization

As mentioned earlier, two cases have been investigated where the vertical structure of the atmosphere is being characterized by high and low values of Richardson number. The other parameters to be specified are the vertical wind shear and mean temperature at one of the levels. By definition of Richardson number, with the usual convention of symbols,

$$R_i = \frac{-\alpha(\partial \ln \theta / \partial p)}{(\partial U / \partial p)^2} \qquad (3)$$

For a 2 level model (Fig. 1) in finite difference form, the above expression may be written as;

$$\bar{\theta}_2 = \bar{\theta}_1 - \frac{R_i}{C_1} \qquad (4)$$

where $C_1 = \dfrac{R}{P_m} \cdot \left(\dfrac{P_m}{P_0}\right)^K \cdot \dfrac{1}{\Delta p} \bigg/ \left(\dfrac{\Delta U}{\Delta P}\right)^2$

and $\bar{\theta}_1$ and $\bar{\theta}_2$ are the potential temperatures at 400 mb and 800 mb respectively, $P_m = 600$ mb, $\Delta p = 400$ mb, $P_0 = 1000$ mb, R is gas constant and $K = .2861$. $\dfrac{\Delta U}{\Delta P}$ has been taken to be equal to 1.0 cm sec^{-1}mb^{-1}, taking $U = -10$ m sec^{-1} at 1000 mb and $U = -4$ m sec^{-1} at 400 mb. This vertical wind structure was specified on the basis of the

analysis presented by Yanai (1961).

Specifying the mean temperature at 400 mb, mean temperature at 800 mb was found by the equation (3). The values of Richardson number in the two cases were taken to be 5 and 100. $R_i = 5$, case is supposed to behave like a baroclinic system where as $R_i = 100$ is expected to be the representative of a barotropic case. Meridional temperature gradients on the isobaric surfaces are computed by making use of the prespecified wind shear and geostrophic relation. Defining σ as follows:

$$\sigma = \frac{p - p_T}{p^* - p_T} \qquad (5)$$

where $p_T = 200$ mb, p^* is surface pressure and p is the pressure at the point under consideration, pressures at the constant sigma surfaces are computed for $\sigma = .75$ and $\sigma = .25$. Knowing the pressures at constant σ surfaces and potential temperatures at 400 mb and 800 mb, potential temperature on σ surfaces are linearly interpolated assuming a constant potential temperature gradient between 800 mb and 400 mb. Knowing the temperatures at the level $\sigma = .25$ and $\sigma = .75$, geopotential heights are computed for the corresponding levels using the integral form of the hydrostatic relation (Mintz, 1964). Thus after obtaining the geopotential field corresponding to the basic easterly current, geopotential field corresponding to the disturbance is added algebraically to get the final geopotential. i.e. $\phi = \bar{\phi} + \phi'$, where $\bar{\phi}$ and ϕ' correspond to the geopotential fields for the basic easterly current and the disturbance respectively. Computation of surface pressure and the disturbance geopotential will be briefly described in the subsequent paragraphs.

Specification of the disturbance : For convenience the sinusoidal disturbance was specified in the geopotential field. The expression for the disturbance may be given as follows:

$$\phi' = A \operatorname{Sin} \frac{2\pi}{L}(x - \alpha) \cdot \operatorname{Sin} \frac{\pi}{D} y \qquad (6)$$

where A = Amplitude of the disturbance
L = Wavelength of the disturbance
D = Lateral dimension of the experimental area

Usually, α is given different values at different levels to introduce some tilt in the trough in vertical, but in the present case α was set equal

to zero. Since the area under consideration had 22×11 grid points and since it was decided to use cyclic boundary condition for east and west boundaries and no inflow or outflow from north and south boundaries, L and D were specified as follows (See Figure 2).
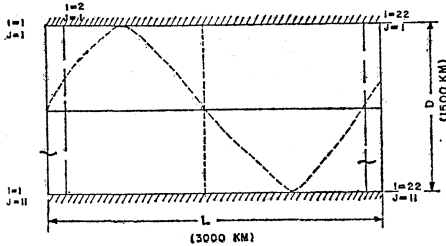

Fig. 2. Schematic representation of the experimental area and the specifications of the disturbance, i.e.,

$$\phi' = A \sin \frac{2\pi}{L}(x-\alpha) \sin \frac{\pi}{D} y$$

$L = 20 \times d$ and $D = 10 \times d$ where $d =$ grid length. Since wavelength was chosen to be 3000 kms., therefore $d = 150$ km. Correspondingly, time step was chosen to be 5 minutes.

Amplitude was calculated by the relations.

$$A = \frac{L}{2\pi} \cdot \frac{\partial \phi'}{\partial x} = \frac{f_0 |V_{max}| \cdot L}{2\pi} \qquad (7)$$

where $|V_{max}|$ was chosen to be 3 m sec^{-1}.

Computation of surface pressure : Surface pressure was computed with the assumption that the mean geopotential height of 1000 mb surface is zero in the middle (latitudinally) of the area. Thus,

$$P_* = \bar{P}_* + P_*'$$

where $\bar{P}_* = 1000$ mb
and $P_*' =$ may be further broken into three components,

$$P_*' = P_g' + P_d' + P_0'$$

where $P_g' =$ Pressure due to the gradient of the geopotential field of 1000 mb surface.
$F_d' =$ Pressure due to the disturbance
$P_0' =$ Pressure due to the orography

In the present case, P_g' was computed by obtaining the gradient of geopotential for 1000 mb surface by making use of geostrophic relation and putting mean easterly current as -10 m sec^{-1} at 1000 mb surface. The corresponding geopotential height was changed into the units of mb by putting

$$4 \text{ mb} = 30 \text{ m}$$

In the present case since, flat ground surface was considered therefore P_0' equals zero. To avoid the complications in transforming the potential temperatures from pressure surfaces to sigma surfaces, initially P_d' was also set equal to zero and it was presumed that by very nature of primitive equations and the time differencing scheme used (Matsuno, 1966) this small discrepancy will be recovered in the course of integration. Surface pressure pattern observed after 24 hours confirmed the anticipated idea.

After getting the geopotential field ϕ on the sigma surfaces, u and v components of the velocities are calculated geostrophically and potential temperature θ is calculated from hydrostatic relation. U, V and θ on the two levels, $\sigma = .75$ and $\sigma = .25$ and P_* are the basic requirements for the time integration of the P.E. model and all other required quantities are calculated by these three variables. Values of U, V, T and P_* are preserved on the history tape at the end of every hour i.e. after every 12 time steps.

3. Description of the model

As schematically shown in Figure 1, a 2-level primitive equation model has been used to perform the experiment. The equations of motion, continuity equation and thermodynamic equation have been used in the following form.

$$\frac{\partial}{\partial t}\left(\frac{\pi u}{mn}\right) + \left|\frac{\partial}{\partial x}\left(\frac{\pi u}{n}u\right) + \frac{\partial}{\partial y}\left(\frac{\pi v}{m}u\right)\right|$$
$$-\frac{1}{n}\frac{\pi v}{m}f^* + \frac{\partial}{\partial\sigma}\left(\frac{\pi\dot{\sigma}}{mn}u\right) + \frac{1}{n}\frac{\partial}{\partial x}(\pi\phi)$$
$$-\frac{1}{n}\left\{\frac{\partial}{\partial\sigma}(\phi\sigma)-\frac{\partial\pi}{\partial x}\right\} - F_x = 0$$

$$\frac{\partial}{\partial t}\left(\frac{\pi v}{mn}\right) + \left|\frac{\partial}{\partial x}\left(\frac{\pi u}{n}v\right) + \frac{\partial}{\partial y}\left(\frac{\pi v}{m}v\right)\right|$$
$$+\frac{1}{m}\frac{\pi u}{n}f^* + \frac{\partial}{\partial\sigma}\left(\frac{\pi\dot{\sigma}}{mn}v\right) + \frac{1}{m}\frac{\partial}{\partial y}(\pi\phi)$$
$$-\frac{1}{m}\left\{\frac{\partial}{\partial\sigma}(\phi\sigma)-\frac{\partial\pi}{\partial y}\right\} - F_y = 0$$

$$\frac{\partial}{\partial t}\left(\frac{\pi}{mn}\right) + \left|\frac{\partial}{\partial x}\left(\frac{\pi u}{n}\right) + \frac{\partial}{\partial y}\left(\frac{\pi v}{m}\right)\right|$$
$$+\frac{\partial}{\partial\sigma}\left(\frac{\pi\dot{\sigma}}{mn}\right) = 0$$

$$\frac{\partial}{\partial t}\left(\frac{\pi\theta}{mn}\right) + \left|\frac{\partial}{\partial x}\left(\frac{\pi u\theta}{n}\right) + \frac{\partial}{\partial y}\left(\frac{\pi v\theta}{m}\right)\right|$$
$$+\frac{\partial}{\partial\sigma}\left(\frac{\pi\dot{\sigma}\theta}{mn}\right) = Q$$

where, $\sigma = \dfrac{p - p_T}{p_s - p_T} = \dfrac{p - p_T}{\pi}$

$$f^* = f + mn\left\{ v \frac{\partial}{\partial x}\left(\frac{1}{n}\right) - u\frac{\partial}{\partial y}\left(\frac{1}{m}\right) \right\}$$

m and n are the map projection factors in x and y direction respectively.

The finite difference scheme and time integration schemes adopted are similar to the one used by Mintz (1964) and Nitta and Hovermale (1967).

Basic assumptions

   i. Frictionless adiabatic atmosphere

   ii. Flat ground surface

   iii. $f = 10^{-5} sec^{-1}$(Constt.) i.e. $\beta = 0$

   iv. $m = n = 1$

   v. Invariance of the disturbance in the vertical

   vi. Vertical wind structure as reported by Yanai (1961).

Boundary condition

No inflow or outflow is allowed from north and south boundaries and cyclic boundary condition is used for east and west boundaries by putting A(1)=A(21) and A(22)=A(2). By putting $D = 10 \times d$ from equation (6), no inflow and outflow is allowed through northern and southern boundaries.

4. Discussion of the results

Equations given in section 3 have been integrated for 24 hours for two sets of input data corresponding to $R_i = 5$ and $R_i = 100$ as discussed in section 2. The following aspects of the behaviour of the disturbance during the course of integration have been examined with a view to understand the contrast between the behaviour of the disturbance characterized by low and high values of Richardson number.

   i. Vertical velocity distribution

   ii. Phase velocity of the disturbance and orientation of the trough axis in vertical

   iii. Time change of kinetic energy as an indicator for energy transformations.

i. Vertical velocity distribution

Figure 3 and 4 give, respectively, the vertical velocity distribution after 24 hours for the two cases characterized by $R_i = 5$ and $R_i = 100$. It is seen that the vertical velocity in the former is quite significant and appreciable vertical coupling can hardly be questioned. For $R_i = 5$, the vertical velocity is one order of magnitude higher than the vertical velocity for $R_i = 100$. The distribution
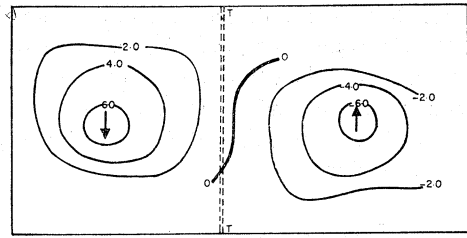

Fig. 3. Vertical velocity (mb/hour) at $\sigma = 0.5$. Richardson number $R_i = 5$; real time of integration NT=24 hours.
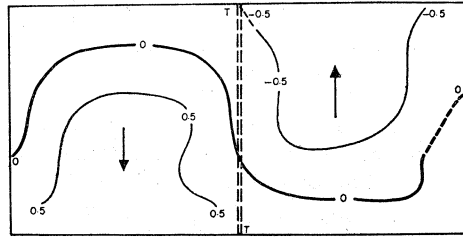

Fig. 4. Vertical velocity (mb/hour) at $\sigma = 0.5$. Richardson number $R_i = 100$; real time of integration NT=24 hours.

of vertical velocity is also quite in agreement with the observed weather distribution associated with tropical easterly disturbance i.e. ascending motion in the rear of the trough and descending motion in front of the troughs.

ii. Phase velocity of the disturbance and orientation of the trough in vertical

Figure 5 gives the schematic representation of the orientation of the trough axis in vertical after 24 hours. It is seen that the tilt in the case of $R_i = 100$ is higher than the tilt in the case of $R_i = 5$. In the case of $R_i = 100$, trough axis in vertical is tilted from east (up) to west (down)
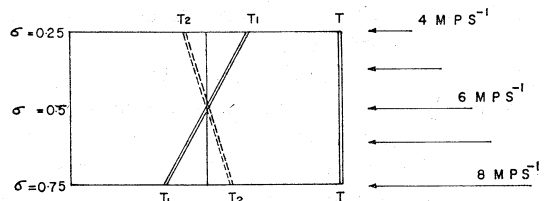

Fig. 5. Schematic representation of the displacement of trough.

   TT : Vertical Orientation of trough at NT=0 hours,

   $T_1 T_1$: at NT=24 hours for $R_i = 100$, (mean speed; 7.0 m/sec),

   $T_2 T_2$: at NT=24 hours for $R_i = 5$, (mean speed; 7.0 m/sec).

indicating a poor vertical coupling because the wind speed of the basic easterly current decreases in vertical. On the other hand, for the same basic easterly current and the same vertical wind shear, the trough axis tilts in vertical from west (up) to east (down). This type of tilt is characteristic of the baroclinic vertically coupled disturbances and it further attests to the validity of the conception of vertical coupling in the case of $R_i = 5$. The magnitude of the tilting was nearly 400 m.mb^{-1} for $R_i = 100$ and nearly 200 m.mb^{-1} for $R_i = 5$. It may be incidentally remarked that similar, against the wind tilting of troughs in vertical, is observed in middle latitude baroclinic westerly disturbances.

iii. Time change of kinetic energy

One of the most important characteristics of the barotropic disturbances is that there is no conversion from potential energy to kinetic energy and hence the rate of change of kinetic energy of the disturbance is quite insignificant, while in the case of baroclinic disturbances, on account of conversion from potential energy to kinetic energy, a significant change in the kinetic energy of the disturbance is expected. In the present study eddy kinetic energy has been calculated at every one hour interval as follows:

Let V_{ij} be the wind velocity at any grid point (i,j). The zonal average $\bar{V}$ is defined as

$$\bar{V}(j) = \frac{1}{M} \sum_{i=1}^{i=M} V(i, j)$$

and $V'(i, j)$ is defined as

$$V'(i, j) = V(i, j) - \bar{V}(j)$$

The eddy kinetic energy per unit area, K' has been calculated by the formula:

$$K' = \frac{1}{M \times N \times K} \left| \sum_i \sum_j \sum_k \left(p_s(i, J) \times \left\{ V'(i, J) \right\}^2 \right)_k \right|$$

where M and N are the number of grid points along x and y axis respectively, and k is the number of levels in vertical.

Figure 6 gives the variation of K' with time. It is seen that in the case of $R_i = 5$, the variation of K' is more than that of the case of $R_i = 100$. In order to make a quantitative comparison between the two cases, percentage change of kinetic energy for 24 hours has been calculated. The percentage change being defined as:

$$P.C. = \frac{K_{24}' - K_0'}{(K_{24}' + K_0')/2} \times 100$$

where K_0' and K_{24}' stand for the initial value of K' and value of K' after 24 hours. It is found that the value of $P.C.$ is nearly 3 for $R_i = 5$ and nearly 0.5 for $R_i = 100$.
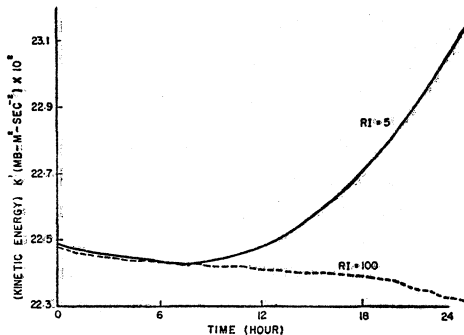

Fig. 6. Time change of kinetic energy for the cases $R_i = 100$ (the dashed line) and 5 (the solid line).

Thus, it further confirms the supposition that in the case of $R_i = 5$, the disturbance behaves like a baroclinic disturbance and there is appreciable vertical coupling. The interesting portion of the tropical flows contain a vertical coupling was earlier stated by Krishnamurthy (1966).

Now, coming to the actual value of static stability or Richardson number for the tropics, it is quite interesting to note that the values are quite small and even negative in the lower and middle
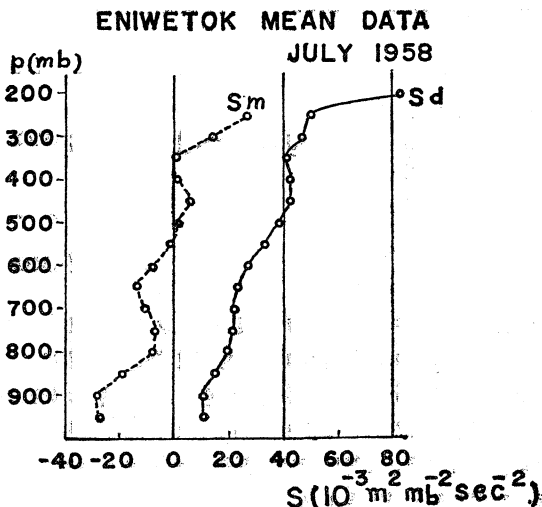

Fig. 7. Vertical profile of the mean monthly value of static stability factor for Eniwetok Island (12.0° N, 162.0°E) for the month of July, 1958 (by Yanai, 1961).

troposphere. Referring to Fig. 7 (reproduced from Yanai, 1961) it is seen that even the mean monthly value of static stability factor for saturated air is negative up to 500 mb for Eniwetok Island (12. 0°N, 162.0°E) for the month of July, 1958. It is also seen from the values of equivalent potential temperatures given by Rao (1958) for different isobaric surfaces for the four month period (June-September) for various stations over India that the static stability factor is negative up to middle troposphere.

Thus, in context with the results of the present numerical experiment, such low and negative values of the observed static stability factor, raise the question: Whether we are justified or not in saying that the tropical disturbances are of barotropic type and have no appreciable vertical coupling.

References

Burger, A., 1958: Scale considerations of planetary motions of the atmosphere. *Tellus*, **10**, 195-205.

Charney, J., 1963: A note on large scale motion in the tropics. *J. atmos. Sci.*, **20**, 607-609.

Krishnamurthy, T.N. and D. Baumhefner, 1966: Structure of a tropical disturbance based on solutions of a multilevel baroclinic model. *J. App. Meteor.*, **5**, 396-406.

Matsuno, T., 1966: Numerical integration of the primitive equation by a simulated backward difference method. *J. meteor. Soc. Japan*, **44**, 76-84,

Mintz, Y., 1964: Very long term global integration of the primitive equations of atmospheric motion. U.C.L.A. Department of Meteorology, Contribution No. 111.

Nitta, T. and J.B. Hovermale, 1967: On analysis and initialization for the primitive forecast equations. *Tech. Mem.* No. 40, National Meteor. Centre, Wash. D.C.

Rao, K.N., 1958: Thermodynamical instability of the upper atmosphere over India during the southwest monsoon. *Symp. on monsoon of the world* held in New Delhi, 43-50.

Yanai, M., 1961: Dynamical aspects of typhoon formation. *Collected meteor. Papers*, **11**, No. 1-2.

—————, 1964: Formation of tropical cyclones. *Reviews of Geophysics*, **2**, No. 2, 367-414..

低緯度偏東風擾乱の発達・減衰に関する数値実験

J. シュクラ

熱帯気象研究所, プーナ

低緯度偏東風中の擾乱の時間変動を, σ-座標系の断熱2層プリミティブ方程式を用いて, 24時間追跡した.

取扱った2例の数値計算では, 擾乱の発達・減衰はリチャードソン数 R_i によって支配される. リチャードソン数が小さい場合, $R_i=5$, では擾乱は発達し, 大きい場合, $R_i=100$, は減衰する. 前者では, 垂直の相互作用が強く, 傾圧性が卓越したことによる. 発達した擾乱の構造は, 偏西風擾乱と似た特長を示している.

本論文で取扱った範囲では, 低緯度大気は Charney のスケール理論で云うように必ずしも順圧的ではなく, 垂直方向の相互作用が重要であるようである.